

Surveying the Scope of the $SU(2)_L$ Scalar Septet Sector

C. Alvarado L. Lehman and B. Ostdiek

*Department of Physics, University of Notre Dame,
225 Nieuwland Science Hall
Notre Dame, IN 46556
USA*

E-mail: calvara1@nd.edu, llehman@nd.edu, bostdiek@nd.edu

ABSTRACT: Extending the Standard Model by adding a scalar field transforming as a septet under $SU(2)_L$ preserves the ρ parameter at tree level and can satisfy experimental constraints on the electroweak parameters S and T . This work presents the first fully general phenomenological study of such an extension. We examine constraints on the septet model couplings based on electroweak and Higgs observables, and use LHC searches for new physics to bound the mass of the septet to be above ~ 400 GeV at a 95% CL.

Contents

1	Introduction	1
2	The Model	2
3	Constraints from observables	5
3.1	<i>S</i> and <i>T</i> Parameters	7
3.2	Higgs to $\gamma\gamma$	8
4	Bounds from the LHC	10
5	Conclusion	14
A	Expanded Potential	15
B	<i>SU</i>(2) Septet Generators	16

1 Introduction

The discovery of the Higgs boson begins a new era in particle physics. We now know many general details about the Higgs, although more precise measurements are needed. Many models of physics beyond the Standard Model (SM) contain more than one scalar which can contribute to breaking the electroweak symmetry. The amount that the scalars mix to create the physical particles can have a large impact on the couplings of the Higgs to both gauge bosons and fermions. Thus, measurements of the production cross section and decay channels of the Higgs offer new constraints on BSM models.

In addition to the new constraints provided by Higgs observables, models are still subject to the electroweak precision observables. The ρ parameter ($\rho \equiv m_W^2/m_Z^2 \cos^2 \theta_W$) measures the ratio of the *W* and *Z* boson masses, which depend on the properties of the Higgs sector. If the scalar sector is comprised only of singlets and doublets, the ρ parameter is equal to one. However, a scalar field transforming as a triplet under $SU(2)_L$ does not preserve $\rho = 1$ at tree level, so experimental constraints force a small vacuum expectation value (vev) of the triplet. For a review of exotic scalar fields see [1, 2].

The general form of the ρ parameter for an $SU(2)_L$ multiplet with weak isospin j_ϕ and hypercharge Y_ϕ is given by

$$\rho = \frac{\sum_\phi (j_\phi(j_\phi + 1) - Y_\phi^2) v_\phi^2}{\sum_\phi (2Y_\phi^2) v_\phi^2}. \quad (1.1)$$

As ρ is measured to be close to 1, the examination of models which protect the value of ρ at tree level is well motivated. After the doublet ($j = 1/2$, $Y = 1/2$), the next $SU(2)_L$

multiplet that leaves ρ unity at tree level is the septet ($j = 3, Y = 2$). In fact, [3] showed that the doublet and the septet are the only multiplets which maintain $\rho = 1$ and preserve perturbative unitarity of scattering amplitudes involving transverse W pairs and pairs of scalars. Interest in the septet has increased since the discovery of the Higgs. Since the septet adds many charged scalars to the Standard Model, it could be used to explain any discrepancy in the observed $h \rightarrow \gamma\gamma$ rate. The authors of [1, 4] examined the production and decays of the observed Higgs for the septet, while [5] explored how the electroweak quantum numbers of an additional scalar field, such as the septet, could be determined through a measurement of the Higgs-Higgs-vector-vector coupling. The sum rules for general scalar representations of $SU(2)_L \times U(1)_Y$ were studied in [6] using perturbative unitarity, including the septet model as a specific example.

One artifact that arises in models containing a scalar with weak isospin $j > 2$ is an accidental $U(1)$ symmetry at the renormalizable level. If the scalar is to develop a vev to contribute to the breaking of the electroweak symmetry, the accidental $U(1)$ symmetry is broken as well. This accidental symmetry cannot be spontaneously broken without generating a phenomenologically unacceptable extra Nambu-Goldstone boson. All such models preserving the $U(1)$ are excluded by dark matter cosmological relic densities and direct-detection cross section via Z exchange [7]. In this paper we are not concerned with dark matter and will thus explicitly break the accidental symmetry with a non-renormalizable operator as done in [4].

This work presents the first constraints on a fully generic septet model with a survey of the parameter space of all possible couplings. Earlier works used simplified scenarios, ignoring certain parameters in the potential. We use the full potential and explicitly calculate electroweak parameters and Higgs observables from the masses and mixings between the doublet and the septet. Using these calculations and the most current experimental results from ATLAS and CMS searches for new physics, we are able to place a general bound on the mass of the septet.

The organization of the paper is as follows. In Section 2 we declare our notation and introduce the model Lagrangian and parameters. Section 3 examines constraints on the septet model from Higgs observables and the S and T parameters. Using LHC searches for new physics, we place bounds on the mass of the septet in Section 4. Section 5 presents our conclusions.

2 The Model

In this section we present an overview of the septet model. This model includes the familiar scalar doublet field, Φ , with quantum numbers $(1/2, 1/2)$ under $SU(2)_L \times U(1)_Y$. In addition, there is a second scalar field, χ , with quantum numbers $(3, 2)$. This is a 7-dimensional representation of $SU(2)$, hence the designation “septet.” These two scalar

fields can be explicitly represented as

$$\Phi = \begin{pmatrix} \phi^+ \\ \phi^0 \end{pmatrix}, \quad \chi = \begin{pmatrix} \chi^{+5} \\ \chi^{+4} \\ \chi^{+3} \\ \chi^{+2} \\ \chi_1^+ \\ \chi^0 \\ \chi_2^- \end{pmatrix}. \quad (2.1)$$

It is important to note that χ_1^+ is not the antiparticle of χ_2^- . When the neutral components of the scalar fields develop vevs, $\langle \phi^0 \rangle \equiv v_2$ and $\langle \chi^0 \rangle \equiv v_7$, mass is given to the W and Z according to the covariant derivatives:

$$m_W^2 = \frac{g^2}{2}(v_2^2 + 16v_7^2), \quad m_Z^2 = \frac{g^2 + g'^2}{2}(v_2^2 + 16v_7^2). \quad (2.2)$$

At tree level, the vev of the septet does not alter the mass of the gauge bosons as long as

$$v^2 = (174 \text{ GeV})^2 = v_2^2 + 16v_7^2, \quad v_2 = v \sin \beta, \quad v_7 = \frac{1}{4}v \cos \beta. \quad (2.3)$$

To remain gauge invariant, the septet field cannot couple to fermions with renormalizable operators. It can also only couple to the doublet through quartic interactions containing each field multiplied by its conjugate. The most general potential is easiest to see using tensor methods [4] and is given by

$$\begin{aligned} V = & m_1^2 \Phi^2 + m_2^2 \chi^2 + \lambda (\Phi^\dagger \Phi)^2 - \frac{1}{\Lambda^3} \{(\chi^* \Phi^5 \Phi^*) + \text{H.C.}\} \\ & + \sum_{A=1}^4 \lambda_A (\chi^\dagger \chi \chi^\dagger \chi)_A + \sum_{B=1}^2 \kappa_B (\Phi^\dagger \Phi \chi^\dagger \chi)_B + \frac{1}{\Lambda^2} \sum_{C=1}^3 \eta_C (\Phi^\dagger \Phi^2 \chi^\dagger \chi)_C. \end{aligned} \quad (2.4)$$

The tensor structure of the potential, with explicit forms for the terms labeled with indices A , B , and C is shown in Appendix A. The λ_A term is a sum over four sub-terms with slightly different tensor structures that collectively give rise to quartic self-interactions of the septet field. Similarly, the κ_B term in (2.4) is a sum over two sub-terms; in this case allowing 4-point interactions between the septet and the doublet. Finally, the η_C term contains three different tensor configurations of a dimension six operator which affects the mass relations of the septet. The dimension-6 η_C term is necessary to maintain consistency of the effective field theory, since we are including the dimension-7 term to break the accidental $U(1)$ symmetry. There are no possible dimension-5 terms.

It will be shown in Section 3 that the LHC Higgs observations force a small value of v_7 . Since v_7 must be small, the septet quartic couplings λ_A will contribute negligibly to the mass of the septet, and the septet three-point interactions will be small. The exact values of the λ_A will thus not have a large effect on this study, as very precise measurements would be needed to determine these values. Another result of v_7 being small is that the possible dimension-6 operators other than η_C either have negligible effects or can be absorbed into λ_A or κ_B .

Keeping in mind that we will later show v_7 to be small, we here show the masses of the septet particles, neglecting the contribution from v_7 and keeping the contributions from m_2 and v_2 .

$$\begin{aligned}
m_{\chi^{+5}}^2 &= m_2^2 + v_2^2(\kappa_1 + \eta_1 \frac{v_2^2}{\Lambda^2}) \\
m_{\chi^{+4}}^2 &= m_2^2 + v_2^2(\kappa_1 + \eta_1 \frac{v_2^2}{\Lambda^2}) + v_2^2 \frac{1}{6}(\kappa_2 + \eta_2 \frac{v_2^2}{\Lambda^2}) \\
m_{\chi^{+3}}^2 &= m_2^2 + v_2^2(\kappa_1 + \eta_1 \frac{v_2^2}{\Lambda^2}) + v_2^2 \frac{1}{3}(\kappa_2 + \eta_2 \frac{v_2^2}{\Lambda^2}) + \eta_3 \frac{v_2^4}{15\Lambda^2} \\
m_{\chi^{++}}^2 &= m_2^2 + v_2^2(\kappa_1 + \eta_1 \frac{v_2^2}{\Lambda^2}) + v_2^2 \frac{1}{2}(\kappa_2 + \eta_2 \frac{v_2^2}{\Lambda^2}) + \eta_3 \frac{v_2^4}{5\Lambda^2} \\
m_{\chi_1^+}^2 &= m_2^2 + v_2^2(\kappa_1 + \eta_1 \frac{v_2^2}{\Lambda^2}) + v_2^2 \frac{2}{3}(\kappa_2 + \eta_2 \frac{v_2^2}{\Lambda^2}) + \eta_3 \frac{2v_2^4}{5\Lambda^2} \\
m_{\chi^0}^2 &= m_2^2 + v_2^2(\kappa_1 + \eta_1 \frac{v_2^2}{\Lambda^2}) + v_2^2 \frac{5}{6}(\kappa_2 + \eta_2 \frac{v_2^2}{\Lambda^2}) + \eta_3 \frac{2v_2^4}{3\Lambda^2} \\
m_{\chi_2^+}^2 &= m_2^2 + v_2^2(\kappa_1 + \eta_1 \frac{v_2^2}{\Lambda^2}) + v_2^2(\kappa_2 + \eta_2 \frac{v_2^2}{\Lambda^2}) + \eta_3 \frac{v_2^4}{\Lambda^2}
\end{aligned} \tag{2.5}$$

Equations (2.4) and (2.5) show that the parameters κ_1 and η_1 couple the septet and doublet equally for each particle. However, the contributions from κ_2 , η_2 , and η_3 increase for lower components of the septet representation. This trend will have a direct impact on the S and T parameters as well as the $h \rightarrow \gamma\gamma$ coupling. We also see that η_1 (η_2) can be reabsorbed into κ_1 (κ_2).

In order to not have the charged components of the septet develop a vev, we do not allow for a negative m_2^2 ; all of the vev of the septet thus comes from the tadpole term of the dimension-7 operator in the first line of (2.4). The fact that this term contains only a single septet field allows for the tadpole and explicitly breaks the accidental $U(1)$ symmetry mentioned in the introduction, thereby preventing a massless Nambu-Goldstone boson. Reference [4] has a more detailed analysis of a possible UV completion leading to this dimension-7 term. Momentarily setting λ_A , κ_B , and η_C in (2.4) to zero gives a septet vev of

$$v_7 = \frac{v_2^6}{\sqrt{6}m_2^2\Lambda^3}. \tag{2.6}$$

As the mass of the septet is decoupled or Λ becomes large, the vev of the septet goes to zero and the Standard Model is recovered. From this point on, we allow λ_A , κ_B , and η_C to vary.

The septet contains two distinct singly charged particles as well as a neutral one. These will mix with the charged and neutral components of the doublet to form physical particles. We define $\Phi_0 = v_2 + (\phi_R^0 + i\phi_I^0)/\sqrt{2}$ and $\chi^0 = v_7 + (\chi_R^0 + i\chi_I^0)/\sqrt{2}$ with the rotations given

Signal	ATLAS	CMS
μ_{WW}	1.25 ± 0.43	0.68 ± 0.20
μ_{ZZ}	1.20 ± 0.58	0.92 ± 0.28
$\mu_{\gamma\gamma}$	1.76 ± 0.50	0.77 ± 0.27
μ_{bb}	0.47 ± 2.17	1.15 ± 0.62
$\mu_{\tau\tau}$	0.44 ± 1.55	1.10 ± 0.41

Table 1: Higgs signal strengths from ATLAS [9] and CMS [10]. The signal strength μ_{xx} is defined as the bound on the Higgs decay rate $\Gamma(h \rightarrow xx)$ divided by the SM expectation.

by

$$\begin{aligned}
\begin{pmatrix} \phi_R^0 \\ \chi_R^0 \end{pmatrix} &= \begin{pmatrix} \cos \alpha & -\sin \alpha \\ \sin \alpha & \cos \alpha \end{pmatrix} \begin{pmatrix} h_0 \\ H_0 \end{pmatrix}, \\
\begin{pmatrix} \phi_I^0 \\ \chi_I^0 \end{pmatrix} &= \begin{pmatrix} \sin \beta & -\cos \beta \\ \cos \beta & \sin \beta \end{pmatrix} \begin{pmatrix} G_0 \\ A_0 \end{pmatrix}, \\
\begin{pmatrix} \phi^+ \\ \chi_1^+ \\ \chi_2^+ \end{pmatrix} &= S_{Charge} \begin{pmatrix} G^+ \\ H_1^+ \\ H_2^+ \end{pmatrix}.
\end{aligned} \tag{2.7}$$

where h_0 is the lightest neutral CP even Higgs and the one observed at the LHC, H_0 is the heavier neutral CP even Higgs, A_0 is the neutral CP odd Higgs, and H_1^+ (H_2^+) is the lighter (heavier) singly charged Higgs. G_0 and G^+ are the goldstones eaten by the W and Z .

3 Constraints from observables

To study the phenomenology of this model we first examine the couplings of the Higgses. The new couplings between the CP-even Higgses and vector bosons are

$$\begin{aligned}
g_{hVV} &= \frac{g^2 v}{\sqrt{2}} (4 \cos \beta \sin \alpha + \cos \alpha \sin \beta) = g_{hVV}^{SM} (4 \cos \beta \sin \alpha + \cos \alpha \sin \beta), \\
g_{HVV} &= \frac{g^2 v}{\sqrt{2}} (4 \cos \alpha \cos \beta - \sin \alpha \sin \beta) = g_{HVV}^{SM} (4 \cos \alpha \cos \beta - \sin \alpha \sin \beta).
\end{aligned} \tag{3.1}$$

Of course, the septet field cannot couple directly to Standard Model fermions. So the Higgs-fermion coupling is only through the doublet:

$$\begin{aligned}
g_{hf\bar{f}} &= \frac{y_f}{\sqrt{2}} \cos \alpha = \frac{m_f}{v_2} \cos \alpha = g_{hf\bar{f}}^{SM} \frac{\cos \alpha}{\sin \beta}, \\
g_{Hf\bar{f}} &= -\frac{y_f}{\sqrt{2}} \sin \alpha = -\frac{m_f}{v_2} \sin \alpha = -g_{hf\bar{f}}^{SM} \frac{\sin \alpha}{\sin \beta}.
\end{aligned} \tag{3.2}$$

From (3.1) and (3.2), note that the SM is recovered as $\alpha \rightarrow 0$ and $\beta \rightarrow \pi/2$.

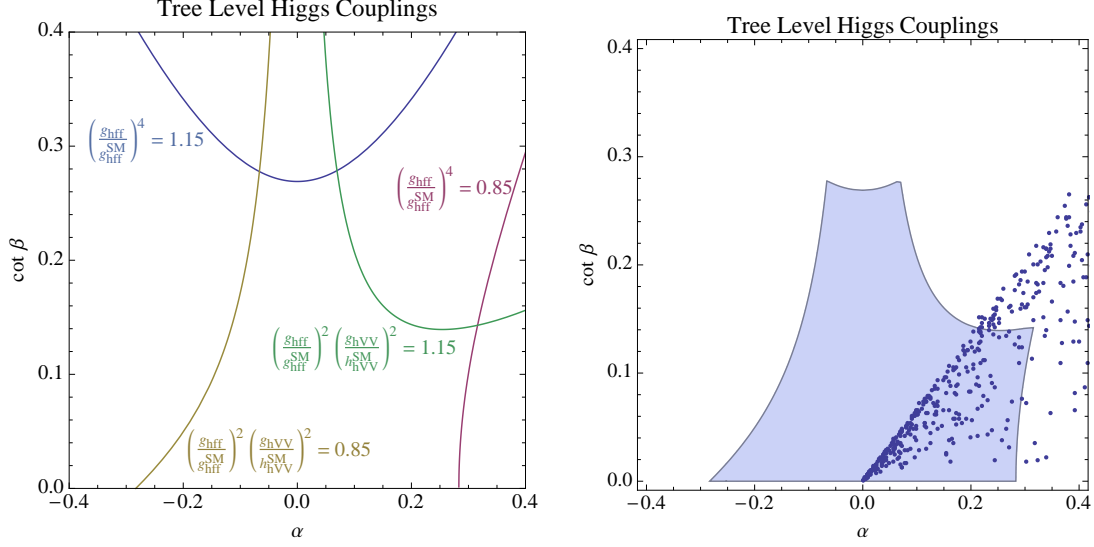


Figure 1: The left panel displays the constraints coming from the tree level Higgs signal strengths. The blue (red) line enforces that gluon fusion followed by a decay to fermions is not too large (small). This is the constraint from (3.3). The yellow (green) lines are for gluon fusion followed by decays to W and Z bosons, which is the constraint shown in (3.4). These constraints set the area of allowed parameter space in α and $\cot \beta$, but the septet model cannot reproduce the observed Higgs mass throughout this entire region. The right panel displays model points chosen with random, perturbative couplings with a minimized potential and $m_h = 125.5$ GeV according to equation (3.5). The shaded area is allowed by the bounds shown in the left panel. To pass the tree level Higgs couplings and generate the correct Higgs mass, the model points must have $\cot \beta \lesssim 0.14$.

Some bounds on the Higgs signal strengths for ATLAS [9] and CMS [10] are shown in Table 1. The signal strengths are the observed rates divided by the SM expectation. In these categories, one experiment measures a value above the SM expectation and the other experiment a value below the SM expectation. We make the conservative assumption that the tree level processes will not deviate from the SM by more than 15 percent. Using this assumption, we make the following cut for gluon fusion with decays to fermions:

$$0.85 \leq \left(g_{h_f \bar{f}} / g_{h_f \bar{f}}^{SM} \right)^4 \leq 1.15. \quad (3.3)$$

A similar cut is made for gluon fusion followed by decays to gauge bosons:

$$0.85 \leq \left(\left(g_{h_f \bar{f}} g_{hVV} \right) / \left(g_{h_f \bar{f}}^{SM} g_{hVV}^{SM} \right) \right)^2 \leq 1.15. \quad (3.4)$$

The left panel of Figure 1 shows the effect of the fermion decay constraints in blue and red, while the gauge boson decays are constrained in green and yellow.

These constraints have come only from the production and decay of the Higgs. These couplings compared to the SM are only determined by the mixing angles of the neutral Higgses and the vevs, with no other assumptions about the masses or couplings in the model. To further constrain the model, we generate random model points which pass constraints (3.3) and (3.4), yield the observed Higgs mass, do not allow for stable charged

scalars, and have perturbative couplings. The model points chosen then have the following form.

$$-2 \leq \{\lambda_1, \lambda_2, \lambda_3, \lambda_4, \kappa_1, \kappa_2, \eta_3\} \leq 2, \quad 0 \leq \cot \beta \leq 0.3, \quad \text{and} \quad 0 \leq m_2 \leq 2 \text{ TeV}. \quad (3.5)$$

At each point, the values of m_1 and Λ are used to minimize the potential and λ sets $m_{h_0} = 125.5$ GeV. The neutral Higgs rotation angle, α is an output of the model. We only keep points which generate α reproducing the allowed Higgs couplings. To satisfy charged dark matter bounds, we assume the mass hierarchy

$$m_{\chi^{5+}} > m_{\chi^{4+}} > m_{\chi^{3+}} > m_{\chi^{2+}}. \quad (3.6)$$

This and the mass relations in (2.5) lead to the assumption that $\kappa_2 \leq 0$. It is possible that three body (or higher) decays could be used to satisfy dark matter bounds if this mass hierarchy is not used. Relaxing this assumption would require an in-depth analysis of actual decay widths and possible charge injection into the early universe. While this is beyond the scope of this paper, a detailed examination of $\kappa_2 > 0$ would be a rich topic of study.

In the right panel of Figure 1 the model points are plotted in the same window as the $(\alpha, \cot \beta)$ tree-level Higgs coupling constraints. It is not possible to generate the observed Higgs mass for all values of $(\alpha, \cot \beta)$. The constraint that the gauge boson signal strengths are not greater than the SM expectation by more than 15% forces $\cot \beta \lesssim 0.14$, or

$$v_7 < 6 \text{ GeV}. \quad (3.7)$$

This small value of v_7 justifies dropping $\mathcal{O}(g^2 v_7^2)$ contributions to the masses given in (2.5).

3.1 S and T Parameters

One of the main motivations of the septet model is that it does not affect the T parameter at tree level ($\alpha T = \rho - 1$). However, it can induce changes at loop level. The scalar contributions to the vacuum polarization at one loop are given by

$$\begin{aligned} \Pi^{AB}(q^2) = \frac{T_{ij}^A T_{ji}^B}{16\pi^2} & \left[(m_i^2 + m_j^2)(1 + \xi) - 2 f_2(m_i, m_j) + 2 m_i^2 (\log m_i^2 - \xi - 1) \right. \\ & \left. + q^2 \left(2 f_1(m_i, m_j) - \frac{\xi}{3} \right) + \mathcal{O}(q^4) \right], \end{aligned} \quad (3.8)$$

where

$$\begin{aligned} f_1(m_i, m_j) &= \int_0^1 dx x(1-x) \log(xm_i^2 + (1-x)m_j^2), \\ f_2(m_i, m_j) &= \int_0^1 dx (xm_i^2 + (1-x)m_j^2) \log(xm_i^2 + (1-x)m_j^2), \\ \xi &= \lim_{\epsilon \rightarrow 0} 2/\epsilon - \gamma + \log 4\pi. \end{aligned}$$

The masses, $m_{(i,j)}$, are given in (2.5) and the $SU(2)_L$ generators for the septet, T_{ij}^A , are given in Appendix B. The S and T parameters are then

$$S = 16\pi [\Pi'^{33}(0) - \Pi'^{3Q}(0)], \quad (3.9)$$

$$T = \frac{4\pi}{s_W^2 c_W^2 m_Z^2} [\Pi^{11}(0) - \Pi^{33}(0)]. \quad (3.10)$$

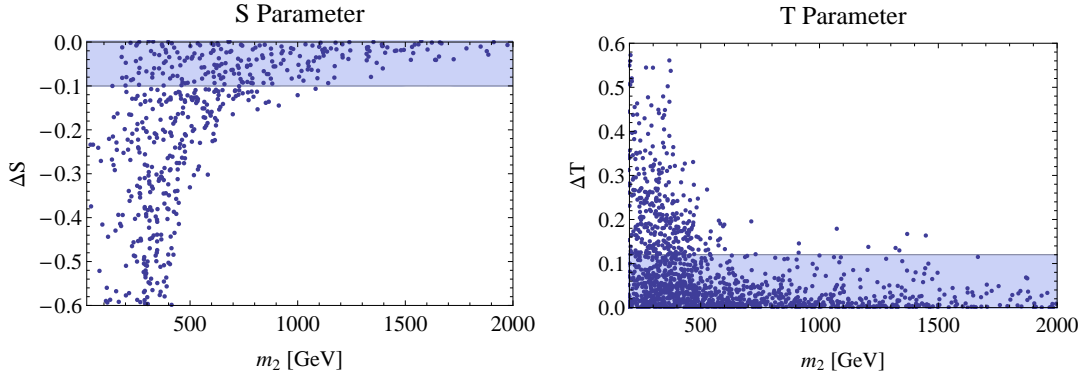


Figure 2: The left (right) panel shows the septet contributions to the S (T) parameter plotted against the septet mass parameter m_2 . The model points are randomly chosen according to equations (3.3), (3.4), and (3.5) such that the observed Higgs mass is generated and the tree-level Higgs couplings do not deviate by more than 15% from the SM value. The shaded area is the allowed region for S and T . At large values of m_2 the contributions to these parameters are small. However, there are still many model points with small values of S and T and low values of m_2 . At low masses the S and T parameters are controlled by κ_2 and η_3 , so these parameters are forced to take values close to zero.

Note that ξ cancels in the calculation so that S and T are finite. The oblique parameters are larger when the mass of different parts of a multiplet are non-degenerate. As v_7 is small from the tree level constraints (3.7), the mass splitting of the septet comes from κ_2 and η_3 , although the η_3 contribution is suppressed by an extra factor of $(v_2/\Lambda)^2$. The contributions to S and T should go to zero as the septet is decoupled. The randomly generated model points contributions to S and T are plotted against the common mass parameter of the septet, m_2 , in figure 2. The shaded box shows the allowed regions [8] where

$$|\Delta S| \leq 0.12 \quad \text{and} \quad |\Delta T| \leq 0.10. \quad (3.11)$$

The septet protects the T parameter at tree level, and the loop contributions are smaller for T than S . For points with $m_2 \gtrsim 600$ GeV the T parameter is small whereas the S parameter is not necessarily small until $m_2 \gtrsim 1$ TeV.

Figure 3 shows the same model points as before with the added condition that $m_2 < 500$ GeV, such that the contributions to S and T can be substantial. If κ_2 is large, the mass splitting among different components of the septet is large, leading to greater contributions to S and T . The mass hierarchy chosen so as to not have a relic abundance of charged septet states has already forced $\kappa_2 \leq 0$ and now the electroweak observables force small values of κ_2 when the mass parameter m_2 is small.

3.2 Higgs to $\gamma\gamma$

The septet model contains many more charged particles coupling to the Higgs than does the SM. The experimental observations of the rate of $h \rightarrow \gamma\gamma$ leave room for non-SM-like behavior. However, CMS measures the rate to be below the SM rate whereas ATLAS measures it to be above, as shown in Table 1. With this in mind, we allow a greater range

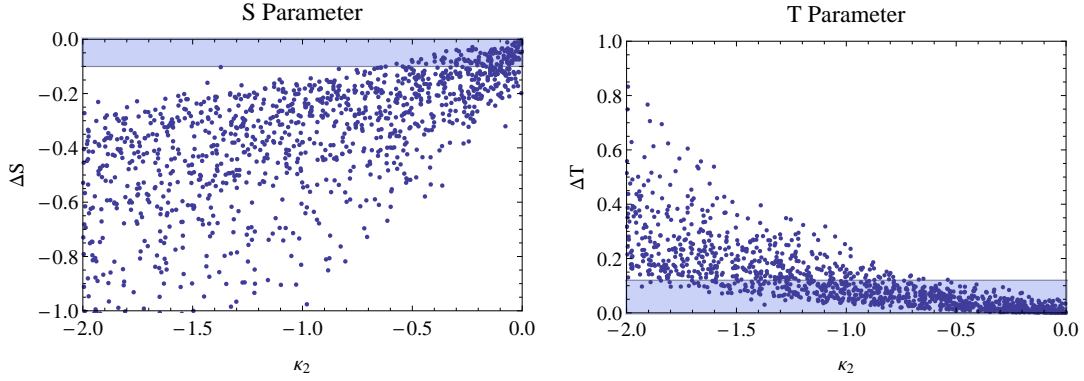


Figure 3: The left (right) panel shows the septet contributions to the S (T) parameter plotted against κ_2 which couples the septet to the doublet in the potential shown in equation (2.4). The model points are randomly chosen according to equations (3.3), (3.4), and (3.5) such that the observed Higgs mass is generated and the tree-level Higgs couplings do not deviate by more than 15% from the SM value. In addition, the model points in this figure have $m_2 < 500$ GeV to allow for large contributions to S and T . The coupling κ_2 alters the mass of the septet differently for each component as seen in equation (2.5). Large absolute values of κ_2 lead to greater mass splitting and thus more contribution to S and T .

for this signal than we did for the gluon fusion signals by only requiring

$$0.5 \leq \Gamma(h \rightarrow \gamma\gamma)/\Gamma(h \rightarrow \gamma\gamma)_{SM} \leq 2.0. \quad (3.12)$$

The partial width of $h \rightarrow \gamma\gamma$ is given by [11] as

$$\Gamma(h \rightarrow \gamma\gamma) = \frac{\alpha^2 m_h^3}{512\pi^3} \left| \frac{g_{hVV}}{m_V^2} Q_V^2 A_1(\tau_V) + \frac{2g_{hf\bar{f}}}{m_f} N_{c,f} Q_f^2 A_{1/2}(\tau_f) + N_{c,s} Q_S^2 \frac{g_{hSS}}{m_S^2} A_0(\tau_S) \right|^2, \quad (3.13)$$

where $v = 174$ GeV, Q is the charge of the particle, N_c is the number of colors, $\tau_x = 4m_x^2/m_h^2$, and the A_S functions are given by

$$\begin{aligned} A_1(x) &= -x^2 (2x^{-2} + 3x^{-1} + 3(2x^{-1} - 1)f(x^{-1})), \\ A_{1/2}(x) &= 2x^2 (x^{-1} + (x^{-1} - 1)f(x^{-1})), \\ A_0(x) &= -x^2 (x^{-1} - f(x^{-1})), \\ f(x) &= \arcsin^2(\sqrt{x}). \end{aligned} \quad (3.14)$$

For the W and top quark, $A_1(\tau_W) = -8.3$ and $A_{1/2}(\tau_t) = 1.4$. If the scalar mass is greater than the Higgs mass $A_0(\tau_S) \sim 1/3$. Thus the scalar contributions work against the SM dominant W boson contributions if the g_{hSS} couplings are positive. This allows the septet to decrease and potentially flip the sign of the $g_{h\gamma\gamma}$ coupling with positive Higgs-septet couplings. If the couplings are negative then the contributions increase the partial decay width. Figure 4 shows the random model points passing the tree-level coupling constraints. Again, the blue shaded region is the allowed region defined by (3.12). As the septet decouples the SM expectation is recovered as shown in the left panel. The tree-level

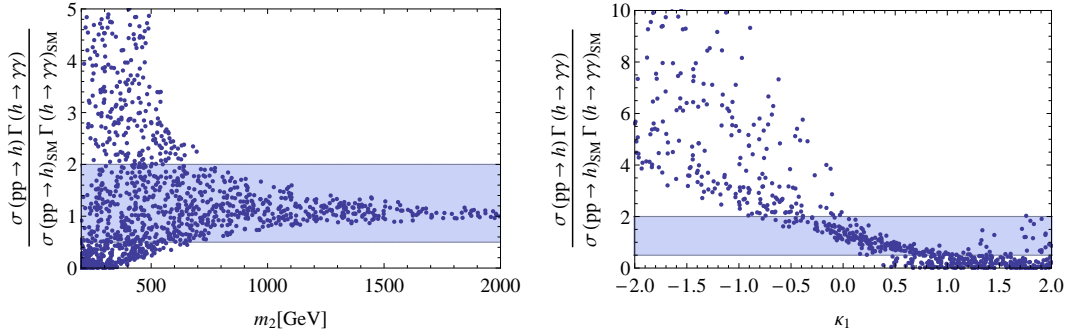


Figure 4: The left panel plots the $h \rightarrow \gamma\gamma$ signal strength of the model points against the septet mass. The model points are randomly chosen according to equations (3.3), (3.4), and (3.5) such that the observed Higgs mass is generated and the tree-level Higgs couplings do not deviate by more than 15% from the SM value. The shaded area corresponds to the allowed region. At large values of m_2 the septet contributions to the $h \rightarrow \gamma\gamma$ signal are small. The coupling of the Higgs to the charged septet fields allowing the di-photon decay comes from the κ_1 , κ_2 , and η_3 terms. At low masses the S and T parameters force small values for κ_2 and η_3 . Because of this, $\Gamma(h \rightarrow \gamma\gamma)$ is affected most by the remaining coupling of the doublet to the septet, κ_1 . The right panel shows the signal strength plotted against κ_1 , for small septet masses ($m_2 < 500$ GeV). A negative value of κ_1 leads to an increase in $\Gamma(h \rightarrow \gamma\gamma)$ while a positive value decreases $\Gamma(h \rightarrow \gamma\gamma)$.

Higgs couplings force a small value of the neutral mixing angle, α . This implies that the observed Higgs is mostly doublet like, therefore the couplings g_{hSS} come from the κ_1 , κ_2 , and η_3 terms. At low masses, S and T force small κ_2 and η_3 . Thus the common coupling of h_0 to the septet, κ_1 , has the most effect on the partial decay width to two photons. A negative value of κ_1 increases $\Gamma(h \rightarrow \gamma\gamma)$ and a positive value decreases it. The right panel shows this trend, where the only model points shown have $m_2 < 500$ GeV. As κ_1 does not affect S and T , any future precise measurement of $h \rightarrow \gamma\gamma$ can be accommodated by the septet model.

4 Bounds from the LHC

After taking all of the constraints from Section 3 into account, the allowed parameter space contains $\cot \beta < 0.14$ and $\alpha < 0.25$. The constraints leading to these bounds all came from electroweak observables or properties of the observed Higgs. The question still remains: how do direct searches for new particles at the LHC constrain the septet model? To answer this question, we create a grid of model points with $0 \leq \cot \beta \leq 0.14$ and $100 \leq m_2 \leq 700$ GeV, with the rest of the model parameters following (3.5). The particular points are chosen to sample the parameter space at very small $\cot \beta$ and provide good coverage for m_2 between 300 and 500 GeV, where the inclusive cross section ranges between hundreds of fb to tens of fb. The grid values are given by

$$\begin{aligned}
 m_2 &= \{100, 200, 300, 350, 400, 450, 500, 600, 700\} \text{ GeV} \\
 \cot \beta &= \{0.001, 0.005, 0.01, 0.02, 0.04, 0.06, 0.08, 0.10, 0.12, 0.14\}.
 \end{aligned}
 \tag{4.1}$$

Each grid point is also forced to follow all of the constraints discussed in Section 3.

As previously noted, the septet model offers a rich landscape of multiply charged particles that can be phenomenologically useful. However, this relatively large number of particles makes a direct search method difficult. For our search, we implemented the septet model in FeynRules [12]. The events were then simulated with MadGraph 5 [13], using Pythia 6.4 [14] for hadronization and PGS [15] for detector simulation.

Using these tools, we considered the production of any new particle pair at the LHC with $\sqrt{s} = 8$ TeV. As the septet does not couple directly to SM fermions or gluons, the production mechanism must be electroweak, going through either a neutral or charged current Drell-Yan type process. It is also possible to create the new particles through VBF leading to four-point interactions with two gauge bosons and two new scalars. The cross section for the VBF process is less than 10% of the total new scalar cross section. The presence of so many new states makes the VBF simulations extremely computationally demanding, so we do not include them in this analysis. Our results are thus conservative, but a dedicated search could find the VBF process useful.

The production of the multiply charged scalars depends only on their quantum numbers, whereas production of the singly charged and neutral components depends on the mixing between the septet and doublet. The W boson couples most strongly to the middle of the representation, while the Z couples most strongly to the top and bottom of the representation. The coupling to the photon is strongest for the particles with the highest charge. With these observations and the mass hierarchy from Eq. (3.6), the order of the cross sections tends to be

$$\begin{aligned} \sigma(pp \rightarrow H_{1,2}^- H_{1,2}^+) &> \sigma(pp \rightarrow \chi^{++} H_{1,2}^-) > \sigma(pp \rightarrow \chi^{+3} \chi^{--}) \\ &> \sigma(pp \rightarrow \chi^{+5} \chi^{5-}) > \sigma(pp \rightarrow \chi^{+4} \chi^{3-}) > \sigma(pp \rightarrow \chi^{+4} \chi^{4-}) > \dots \end{aligned} \quad (4.2)$$

where the choice of (1, 2) depends on the mixing involved. Due to the mixing in both the singly charged and the neutral components, (4.2) is not completely general. The ordering of the cross sections of the neutral and singly charged particles may slightly change among themselves as well compared to the ordering with the multiply charged states. However, the ordering of the multiply charged states with respect to other multiply charged states will remain constant. The large quantum numbers and sheer number of states in the septet leads to relatively large inclusive cross sections. For example, with $m_2 \sim 250$ GeV the cross section is on the order of a pb. In comparison the production of the much lighter W^+W^- at $\sqrt{s} = 8$ TeV is ~ 35 pb. The total cross section in fb of all combinations of septet pairs is shown in Figure 5.

The decay of a multiply charged state goes to the next lowest charged state and either a W or a singly charged Higgs. However, the septet states tend to be nearly degenerate so the W or charged Higgs will be off-shell. The doubly charged scalar can decay to two W bosons, or a W and a singly charged Higgs. The dominant decay depends on the masses as well as α and β . Once the decay chain reaches the neutral septet state, the decay will have to continue through mixing with the neutral doublet. As $\cot \beta \rightarrow 0$ and $\alpha \rightarrow 0$ the H_0 couplings to fermions and gauge bosons go to zero as seen in (3.1) and (3.2), leading to a stable particle at the end of the decay chain. As mentioned before, [7] shows that models

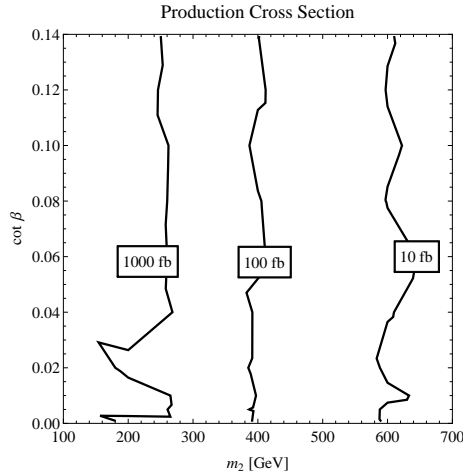


Figure 5: The total cross section in fb of the production of all possible pairs of septet particles.

such as these can be ruled out from a dark matter perspective. However, even at our smallest value of $\cot \beta = 0.001$, the width of H_0 is large enough to decay instantaneously. We again ignore the dark matter constraint and only study the collider results.

Due to the relative strength of the production of multiply charged particles and their decays, the search strategy will be to look for many W s. If the W decays leptonically, the lepton is easy to identify, and the neutrino leads to missing energy. The other option is to have hadronic W decays, producing many jets.

For each of the 90 model points in the grid, we simulate proton-proton collisions at $\sqrt{s} = 8$ TeV. We then employ the same search strategies as done by the CMS and ATLAS experiments. The searches used are: the CMS search for anomalous production of events with three or more leptons [16]; the ATLAS search for strongly produced SUSY particles in final states with two same sign leptons and jets [17]; the ATLAS search for charginos and neutralinos in events with three leptons and missing transverse momentum [18]; and the ATLAS search for squarks and gluinos in final states with jets and missing transverse momentum and no leptons [19].

We use the experimental search data to calculate the 95% CL limit on the number of allowed events in a particular bin, denoted by $s_{i,95}$. To compute $s_{i,95}$, we use the SM expected number of events (b_i), the error in the SM expected number ($\sigma_{b,i}$), and the number of events observed by the experiment (n_i). These values are plugged into the following equation, which is then numerically solved for $s_{i,95}$:

$$\frac{\int \delta b_i \text{Gaus}(\delta b_i, \frac{\sigma_{b,i}}{b_i}) \times \text{Pois}(n_i | b_i(1 + \delta b_i) + s_{i,95})}{\int \delta b_i \text{Gaus}(\delta b_i, \frac{\sigma_{b,i}}{b_i}) \times \text{Pois}(n_i | b_i(1 + \delta b_i))} = 0.05. \quad (4.3)$$

To compute the expected limit instead of the observed limit, b_i is used in place of n_i . Using the Gaussian distribution is an attempt to take into account the uncertainties. However, many of the ATLAS papers present their own values for $s_{i,95}$, which include systematics and other uncertainties. In all such cases, our calculation of $s_{i,95}$ resulted in a larger value than that given by ATLAS. A larger value means that more signal events are required to

Signal Region	Cuts	Observed	SM Expected	Error	Expected $s_{i,95}$	Observed $s_{i,95}$
ATLAS-CONF 2013-007 SR0b	0 b-jets $N_{jets} \geq 3$ $E_T^{\text{miss}} > 150$ GeV	5	7.5	3.3	11.7	8.6
Two same sign leptons	$m_T > 100$ GeV $m_{eff} > 400$ GeV					
ATLAS-CONF 2013-035 SRnoZc	$m_{SFOS} < 81.2$ GeV or $m_{SFOS} > 101.2$ GeV $E_T^{\text{miss}} > 75$ GeV	5	4.4	1.8	8.6	9.5
Three leptons	$m_T > 100$ GeV $p_T^{3^{\text{rd}}\ell} > 30$ GeV					

Table 2: Experimental search bins which are the most constraining bin for the greatest number of model points. These two bins were the most significant for $\sim 2/3$ of the model points tested. The transverse mass is defined as $m_T = \sqrt{2 \cdot E_T^{\text{miss}} \cdot p_T^\ell \cdot (1 - \cos \Delta\phi_{\ell, E_T^{\text{miss}}})}$. The variable m_{eff} is the scalar sum of the transverse momentum of the two leptons. For the three lepton search, m_{SFOS} is the invariant mass of the same flavor opposite sign lepton pair which is closest to the Z mass.

exclude a model point at the 95% CL. We therefore use our numbers, calculated with (4.3), in order to remain conservative and to keep a consistent statistical method between the searches that present values for $s_{i,95}$ and those that do not.

The number of events in a given bin is a function of the luminosity, the cross section, and the acceptance

$$s_i = \mathcal{L} \sigma_i \epsilon_i. \quad (4.4)$$

The detector simulations from PGS give the acceptance for each bin (ϵ_i) which can be used with the maximum number of events allowed, $s_{i,95}$, to find the cross section which is excluded at the 95% CL. The total production cross section of each model point is compared to the bin which constrains the cross section to the smallest value. The model point is excluded if the cross section is larger than this value.

When computing the *expected* limits on the cross section, around 2/3 of the model points are most limited by the three lepton search. In this search all same flavor opposite sign lepton pairs are required to be away from the Z mass and contain large amounts of missing energy. The transverse momentum of the non-paired lepton is required to be above 30 GeV, and the transverse mass is required to be above that of the W mass. The transverse mass is defined as $m_T = \sqrt{2 \cdot E_T^{\text{miss}} \cdot p_T^\ell \cdot (1 - \cos \Delta\phi_{\ell, E_T^{\text{miss}}})}$. Most of the other model points are most constrained by a search for two same sign leptons. The two same sign lepton search requires more missing energy and at least three jets none of which are tagged as b-jets. The transverse mass of the leading lepton is again required to be above the mass of the W . Finally, the scalar sum of the transverse momentum of both leptons must be greater than 400 GeV. The cut information for these bins is shown in Table 2. The observed number of events passing the two lepton search is less than expected, which leads to a lower allowed cross section for new physics. Thus, when computing the *observed*

limits, the two same sign lepton search is most limiting for most of the events, followed by the three lepton search.

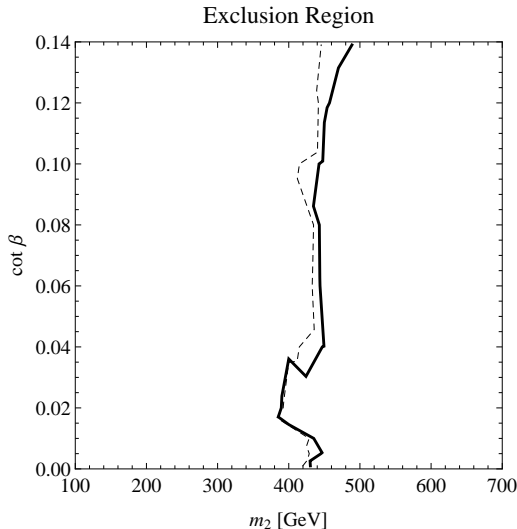


Figure 6: A combination of ATLAS and CMS experimental searches for BSM physics have been used to constrain the mass of the septet for fixed values of the mixing angle (β) of the vevs of the septet and the doublet. All model points follow the constraints from section 3, specifically the tree level Higgs couplings do not change by more than 15%, the $h \rightarrow \gamma\gamma$ rate is consistent with observation, and the one loop contributions to the oblique S and T parameters are within experimental limits. The limits are calculated by considering allowed cross section for every bin and taking the smallest for each model point. The allowed cross section is obtained using equation (4.4) where $s_{i,95}$ comes from equation (4.3). The dashed line represents the expected limit while the solid line is the observed limit. The model points to the left of the lines have a larger cross section than allowed by the experimental searches and are thus excluded. From this we have shown that LHC searches rule out a mass of the septet below about 400 GeV.

Figure 6 shows the limits coming from the most limiting bin at each model point. The dashed line is the expected limit, and follows the expected limit from the three lepton search. The solid line is the observed limit, which follows that of the two same sign lepton search. The area to the left of the lines has a larger cross section than allowed by the searches and is excluded. From this we rule out a mass parameter for the septet (m_2) below ~ 400 GeV at the 95% CL.

5 Conclusion

We have presented a phenomenological study of a general scalar septet extension to the Standard Model, and shown that septet masses are excluded below about 400 GeV at the 95% CL. This constraint came from using ATLAS and CMS searches for BSM physics. The search for two same sign leptons gave the best observed limit followed closely by a three lepton search. The three lepton search gave the best expected limit. The 400 GeV bound on m_2 is still low enough that S and T are not guaranteed to be small, which happens closer to 1 TeV. This in turn forces small values of κ_2 , which is responsible for separating

the mass of the different components of the septet. Having a small value of κ_2 then allows the other doublet-septet coupling, κ_1 to determine the $h \rightarrow \gamma\gamma$ rate. For $m_2 \sim 400$ GeV, a choice of κ_1 between -2 and 2 allows for a range of $h \rightarrow \gamma\gamma$ from 0 to above 10 times the standard model rate. Even if the mass of the septet is pushed to 1 TeV, the septet model has enough charged particles coupling to the Higgs that κ_1 has freedom to match a future more precise measurement of the diphoton coupling.

Acknowledgements This research was supported in part by the Notre Dame Center for Research Computing through computing resources. We thank Joseph Bramante, Antonio Delgado, Adam Martin, and James Unwin for enlightening discussions. This work was partly supported by the National Science Foundation under grant PHY-1215979.

Appendix A Expanded Potential

As a reminder, the potential is given by

$$\begin{aligned}
V = & m_1^2 \Phi^2 + m_2^2 \chi^2 + \lambda (\Phi^\dagger \Phi)^2 - \frac{1}{\Lambda^3} \{ (\chi^* \Phi^5 \Phi^*) + \text{H.C.} \} \\
& + \sum_{A=1}^4 \lambda_A (\chi^\dagger \chi \chi^\dagger \chi)_A + \sum_{B=1}^2 \kappa_B (\Phi^\dagger \Phi \chi^\dagger \chi)_B + \frac{1}{\Lambda^2} \sum_{C=1}^3 \eta_C (\Phi^\dagger {}^2 \Phi^2 \chi^\dagger \chi)_C.
\end{aligned} \tag{A.1}$$

For completeness, we here show the explicit tensor structure of the terms (summation over repeated indices is assumed).

$$\begin{aligned}
(\chi^\dagger \chi \chi^\dagger \chi)_1 &= \chi^*{}^{ijklmn} \chi_{ijklmn} \chi^*{}^{abcdef} \chi_{abcdef} \\
(\chi^\dagger \chi \chi^\dagger \chi)_2 &= \chi^*{}^{ijklmn} \chi_{ijklmf} \chi^*{}^{abcdef} \chi_{abcden} \\
(\chi^\dagger \chi \chi^\dagger \chi)_3 &= \chi^*{}^{ijklmn} \chi_{ijklef} \chi^*{}^{abcdef} \chi_{abcdmn} \\
(\chi^\dagger \chi \chi^\dagger \chi)_4 &= \chi^*{}^{ijklmn} \chi_{ijkdef} \chi^*{}^{abcdef} \chi_{abclmn} \\
(\Phi^\dagger \Phi \chi^\dagger \chi)_1 &= \Phi^*{}^i \Phi_i \chi^*{}^{abcdef} \chi_{abcdef} \\
(\Phi^\dagger \Phi \chi^\dagger \chi)_2 &= \Phi^*{}^i \Phi_j \chi^*{}^{jabcde} \chi_{iabcde} \\
(\chi^* \Phi^5 \Phi^*) &= \chi^*{}^{abcdef} \Phi_a \Phi_b \Phi_c \Phi_d \Phi_e \Phi^{*g} \epsilon_{fg} \\
(\Phi^\dagger {}^2 \Phi^2 \chi^\dagger \chi)_1 &= \Phi^*{}^i \Phi_i \Phi^*{}^j \Phi_j \chi^*{}^{abcdef} \chi_{abcdef} \\
(\Phi^\dagger {}^2 \Phi^2 \chi^\dagger \chi)_2 &= \Phi^*{}^i \Phi_i \Phi^*{}^j \Phi_k \chi^*{}^{kbcdef} \chi_{jbcdef} \\
(\Phi^\dagger {}^2 \Phi^2 \chi^\dagger \chi)_3 &= \Phi^*{}^i \Phi_k \Phi^*{}^j \Phi_l \chi^*{}^{lkcdef} \chi_{ijcdef}
\end{aligned} \tag{A.2}$$

The field definitions in the tensor method are as follows.

$$\begin{aligned}
\chi^{111111} &= \chi^{+5} \\
\chi^{211111} &= \chi^{+4} / \sqrt{6} \\
\chi^{221111} &= \chi^{+3} / \sqrt{15} \\
\chi^{222111} &= \chi^{++} / 2\sqrt{15}. \\
\chi^{222211} &= \chi_1^+ / \sqrt{15} \\
\chi^{222221} &= \chi^0 / \sqrt{6} \\
\chi^{222222} &= \chi_2^-
\end{aligned} \tag{A.3}$$

Appendix B $SU(2)$ Septet Generators

The septet is a $(3,2)$ under $SU(2)_L \times U(1)_Y$. For convenience, the generators for the 7-dimensional representation of $SU(2)$ are listed below, along with $Q = T_3 + Y$.

$$T_1 = \frac{1}{\sqrt{2}} \begin{pmatrix} 0 & \sqrt{3} & 0 & 0 & 0 & 0 & 0 \\ \sqrt{3} & 0 & \sqrt{5} & 0 & 0 & 0 & 0 \\ 0 & \sqrt{5} & 0 & \sqrt{6} & 0 & 0 & 0 \\ 0 & 0 & \sqrt{6} & 0 & \sqrt{6} & 0 & 0 \\ 0 & 0 & 0 & \sqrt{6} & 0 & \sqrt{5} & 0 \\ 0 & 0 & 0 & 0 & \sqrt{5} & 0 & \sqrt{3} \\ 0 & 0 & 0 & 0 & 0 & \sqrt{3} & 0 \end{pmatrix} \quad (\text{B.1})$$

$$T_2 = \frac{i}{\sqrt{2}} \begin{pmatrix} 0 & -\sqrt{3} & 0 & 0 & 0 & 0 & 0 \\ \sqrt{3} & 0 & -\sqrt{5} & 0 & 0 & 0 & 0 \\ 0 & \sqrt{5} & 0 & -\sqrt{6} & 0 & 0 & 0 \\ 0 & 0 & \sqrt{6} & 0 & -\sqrt{6} & 0 & 0 \\ 0 & 0 & 0 & \sqrt{6} & 0 & -\sqrt{5} & 0 \\ 0 & 0 & 0 & 0 & \sqrt{5} & 0 & -\sqrt{3} \\ 0 & 0 & 0 & 0 & 0 & \sqrt{3} & 0 \end{pmatrix} \quad (\text{B.2})$$

$$T_3 = \begin{pmatrix} 3 & 0 & 0 & 0 & 0 & 0 & 0 \\ 0 & 2 & 0 & 0 & 0 & 0 & 0 \\ 0 & 0 & 1 & 0 & 0 & 0 & 0 \\ 0 & 0 & 0 & 0 & 0 & 0 & 0 \\ 0 & 0 & 0 & 0 & -1 & 0 & 0 \\ 0 & 0 & 0 & 0 & 0 & -2 & 0 \\ 0 & 0 & 0 & 0 & 0 & 0 & -3 \end{pmatrix} \quad (\text{B.3})$$

$$Q = \begin{pmatrix} 5 & 0 & 0 & 0 & 0 & 0 & 0 \\ 0 & 4 & 0 & 0 & 0 & 0 & 0 \\ 0 & 0 & 3 & 0 & 0 & 0 & 0 \\ 0 & 0 & 0 & 2 & 0 & 0 & 0 \\ 0 & 0 & 0 & 0 & 1 & 0 & 0 \\ 0 & 0 & 0 & 0 & 0 & 0 & 0 \\ 0 & 0 & 0 & 0 & 0 & 0 & -1 \end{pmatrix} \quad (\text{B.4})$$

References

- [1] S. Kanemura, M. Kikuchi and K. Yagyu, “Probing exotic Higgs sectors from the precise measurement of Higgs boson couplings,” *Phys. Rev. D* **88**, no. 1, 015020 (2013) [arXiv:1301.7303 [hep-ph]].
- [2] K. Yagyu, “Higgs sectors with exotic scalar fields,” arXiv:1304.6338 [hep-ph].
- [3] K. Hally, H. E. Logan and T. Pilkington, “Constraints on large scalar multiplets from perturbative unitarity,” *Phys. Rev. D* **85**, 095017 (2012) [arXiv:1202.5073 [hep-ph]].

- [4] J. Hisano and K. Tsumura, “Higgs boson mixes with an SU(2) septet representation,” *Phys. Rev. D* **87**, 053004 (2013) [arXiv:1301.6455 [hep-ph]].
- [5] R. Killick, K. Kumar and H. E. Logan, “Learning what the Higgs boson is mixed with,” *Phys. Rev. D* **88**, 033015 (2013) [arXiv:1305.7236 [hep-ph]].
- [6] B. Grinstein, C. W. Murphy, D. Pirtskhalava and P. Uttayarat, “Theoretical Constraints on Additional Higgs Bosons in Light of the 126 GeV Higgs,” arXiv:1401.0070 [hep-ph].
- [7] K. Earl, K. Hartling, H. E. Logan and T. Pilkington, “Constraining models with a large scalar multiplet,” *Phys. Rev. D* **88**, no. 1, 015002 (2013) [arXiv:1303.1244 [hep-ph]].
- [8] M. Baak, M. Goebel, J. Haller, A. Hoecker, D. Kennedy, R. Kogler, K. Moenig and M. Schott *et al.*, “The Electroweak Fit of the Standard Model after the Discovery of a New Boson at the LHC,” *Eur. Phys. J. C* **72**, 2205 (2012) [arXiv:1209.2716 [hep-ph]].
- [9] G. Aad *et al.* [ATLAS Collaboration], “Observation of a new particle in the search for the Standard Model Higgs boson with the ATLAS detector at the LHC,” *Phys. Lett. B* **716**, 1 (2012) [arXiv:1207.7214 [hep-ex]].
- [10] S. Chatrchyan *et al.* [CMS Collaboration], “Observation of a new boson with mass near 125 GeV in pp collisions at $\sqrt{s} = 7$ and 8 TeV,” *JHEP* **1306**, 081 (2013) [arXiv:1303.4571 [hep-ex]].
- [11] M. Carena, I. Low and C. E. M. Wagner, “Implications of a Modified Higgs to Diphoton Decay Width,” *JHEP* **1208**, 060 (2012) [arXiv:1206.1082 [hep-ph]].
- [12] A. Alloul, N. D. Christensen, C. Degrande, C. Duhr and B. Fuks, “FeynRules 2.0 - A complete toolbox for tree-level phenomenology,” arXiv:1310.1921 [hep-ph].
- [13] J. Alwall, M. Herquet, F. Maltoni, O. Mattelaer and T. Stelzer, “MadGraph 5 : Going Beyond,” *JHEP* **1106**, 128 (2011) [arXiv:1106.0522 [hep-ph]].
- [14] T. Sjostrand, S. Mrenna and P. Z. Skands, “PYTHIA 6.4 Physics and Manual,” *JHEP* **0605** (2006) 026 [hep-ph/0603175].
- [15] <http://www.physics.ucdavis.edu/~conway/research/software/pgs/pgs4-general.htm>
- [16] CMS Collaboration [CMS Collaboration], “A search for anomalous production of events with three or more leptons using 19.5/fb of $\sqrt{s}=8$ TeV LHC data,” CMS-PAS-SUS-13-002.
- [17] [ATLAS Collaboration], “Search for strongly produced superpartners in final states with two same sign leptons with the ATLAS detector using 21 fb⁻¹ of proton-proton collisions at $\sqrt{s}=8$ TeV.,” ATLAS-CONF-2013-007.
- [18] [ATLAS Collaboration], “Search for direct production of charginos and neutralinos in events with three leptons and missing transverse momentum in 21 fb⁻¹ of pp collisions at $\sqrt{s} = 8$ TeV with the ATLAS detector,” ATLAS-CONF-2013-035.
- [19] [ATLAS Collaboration], “Search for squarks and gluinos with the ATLAS detector in final states with jets and missing transverse momentum and 20.3 fb⁻¹ of $\sqrt{s} = 8$ TeV proton-proton collision data,” ATLAS-CONF-2013-047.